A comparative study of the photo-catalytic performance of amorphous and nano-crystalline TiO_2

A. MOLEA, V. POPESCU*, N. A. ROWSON[a]
Technical University of Cluj-Napoca, Faculty of Material and Environmental Engineering, Physics and Chemistry Department, No.103-105 Muncii avenue, 400641 Cluj-Napoca, Romania
[a]*University of Birmingham, School of Chemical Engineering, Edgbaston Birmingham B15 2TT, United Kingdom*

Titanium dioxide powders with photocatalytic properties were obtained by a simple hydrolysis method, using an inorganic precursor. The effect of the annealing temperature on the formation and subsequent photocatalytic activity has been studied. The powders were characterized by X-ray diffraction, Raman and UV-Vis spectrometry in order to emphasise the structural and optical properties. The photo-catalytic performance of the powders by degradation of Methylene Blue under low intensity UVA and visible radiation were also quantified. The amorphous powder exhibits higher photo-catalytic activity than the equivalent anatase phase. The degradation efficiency of the dye in presence of the amorphous catalyst was 43%.

(Received September 6, 2014; accepted March 19, 2015)

Keywords: TiO_2 catalyst, Amorphous, Nano-crystalline phases, Photo-catalytic performance

1. Introduction

The photocatalytic activity of amorphous TiO_2 has rarely been studied because according with many researchers [1-3], the amorphous phase of TiO_2 facilitates the recombination of the electron-hole pair, which leads to a decrease in photo-catalytic activity. However, Zou et al [4] studied the photo-catalytic activity of amorphous TiO_2 sol by degradation of Methylene Blue (MB), in the absence and presence of hydrogen peroxide and noticed that the efficiency of the photodegradation process was 13% and 90% respectively, after 120 minutes under ultraviolet irradiation, using a 40W UV lamp. A high photocatalytic activity of amorphous TiO_2 sol sensitized with H_2O_2 facilitated the physisorption of water molecules on the catalyst surface, which resulted in the generation of more OH• radicals [4]. Wang et al [5] synthesised amorphous TiO_2 at room temperature by the hydrolysis of $Ti(OBu)_4$ in water and studied the photo-catalytic performance of the powder by the removal of Cr(VI) and Rhodamine B (RhB) dye under visible light irradiation (500W). The best results were obtained after 100 min irradiation with visible light; the efficiency for degradation of RhB and reduction of Cr(VI) in presence of the amorphous TiO_2 was 97.8% and 53.5%, respectively [5].

In this study, amorphous and nano-crystalline titanium dioxide powders were synthesised by a simple hydrolysis technique using titanium tri-chloride. Inorganic $TiCl_3$ was used as a precursor because when using organic precursors, as a titanium source, is difficult to remove any organic residues from the particle surface [6]. The photo-catalytic activity of the synthesised powders was quantified by the degradation of Methylene Blue under low intensity UVA and visible radiation.

2. Materials and method

2.1 Synthesis of TiO_2 powders at different temperatures

Titanium dioxide powders were synthesised by the hydrolysis of titanium tri-chloride $TiCl_3$ 10 % (5 ml) in distilled water, in the presence of hydrogen peroxide 3% (5 ml). The pH was adjusted to 8.5 with 15 ml NH_4OH. The precipitates obtained were filtered, washed with distilled water and heat treated at 200 ^{0}C, 400 ^{0}C, 600 ^{0}C and 800 ^{0}C, respectively, for 1 hour.

2.2 Characterisation

X-ray diffraction patterns were collected using a Bruker AXS D8 diffractometer working with CuKα radiation (λ= 1.5406 Å). The patterns were evaluated using Powder Cell software [7].

Raman spectra of specimens were registered using a WiTec Alpha 300 R (LOT Oriel, UK) operating a 0.3 W single frequency 785 nm diode laser (Toptica Photonics, Germany) and an Acton SP2300 triple grating monochromator/spectrograph (Princeton Instruments, USA). A Confocal Raman spectroscope was used to identify the fundamental Raman vibration for the TiO_2 crystalline phases.

A Lambda 35 UV-Vis spectrometer with an integrated sphere was used to determine the optical properties of the TiO_2 powders. The total transmittance of the samples was measured. Based on UV-Vis measurements the energy band gap (E_g) of the samples was determined using Tauc's relation [8]:

$$\alpha h\nu = A\left(h\nu - E_g\right)^m \quad (1)$$

where: α is the absorption coefficient, hν is photon energy, A is an energy dependent constant and m is an integer depending on the nature of electronic transitions. For the direct allowed transitions, m has a value of 1/2 while for indirect allowed transitions, m=2 [8]. The absorption coefficient α was calculated with the formula [9]:

$$\alpha = 2.303 \cdot \frac{10^3 A \cdot \rho}{c \cdot l} \quad (2)$$

where: A is the absorbance, ρ is the bulk TiO_2 density (ρ=3.84 [g/cm^3]), c is the concentration of the TiO_2 suspensions (c=1.2·10^{-3} [g/cm^3]), and l is the path length (l=1 [cm]).

The Urbach energy (E_U) and the absorption edge have been determined [10]. The values obtained were correlated with the structural parameters. For the determination of E_U the following equation was used [10]:

$$\alpha = \alpha_0 \exp\left(\frac{h\nu}{E_U}\right) \quad (3)$$

where: α is the absorption coefficient, α_0 is a constant. E_u was determined from the slop of the plot lnα versus (hν) [10].

2.3 Photodegradation experiment

In order to assess the photo-catalytic activity performance of the synthesised powders, Methylene Blue dye was degraded, under both UVA and visible radiation, emitted by two lamps: 6W UVA lamp (300-400nm) and 9W visible lamp (400-700nm). The lamps were used in order to mimic solar radiation. The experiment took place at room temperature. A volume of 50 ml photocatalyst suspension, which contains 0.01 g catalyst, was mixed with 50 ml Methylene Blue solution ~5.5×10^{-3} mg/ml. The mixture was maintained under dark conditions for 1 hour, in order to establish the adsorption/desorption equilibrium, followed by irradiation for 300 minutes with both UVA and visible radiation. The intensity of the radiation (measured with Digitales Mavolux 5032C Luxmeter) at the samples surface was 0.183 mW/cm^2. A sample without catalyst was prepared as blank.

The variation of the Methylene Blue concentration as a function of the irradiation time was determined using the UV-Vis spectroscopy using a calibration curve of the Methylene Blue dye. Based on experimental data, the efficiency of the degradation process was calculated with the relation [11]:

$$\text{Efficiency } \% = \frac{C_{Mb}^0 - C_{Mb}}{C_{Mb}^0} \cdot 100 \quad (4)$$

where: $C_{MB}{}^0$ is the initial concentration of Methylene Blue and C_{MB} is the concentration of Methylene Blue at a given irradiation time. At low concentrations of dye, the photodegradation reactions exhibited a first order kinetic mechanism [12,13]. Based on the results, the kinetics of the degradation process of Methylene Blue and the rate constant, k, were studied. The rate constant was obtained by plotting the logarithm of the ratio between the initial concentration ($C_{MB}{}^0$) and the concentration at a given irradiation time (C_{MB}) Methylene Blue, versus irradiation time [12]:

$$-\ln\frac{c_{MB}^0}{c_{MB}} = kt \quad (5)$$

where: k is the rate constant and t is the irradiation time.

3. Results and discussion

3.1 X-ray diffraction

XRD patterns of the TiO_2 powders obtained in alkaline medium and annealed at different temperatures (200 ^{0}C, 400 ^{0}C, 600 ^{0}C and 800 ^{0}C, respectively) are shown in Fig. 1.

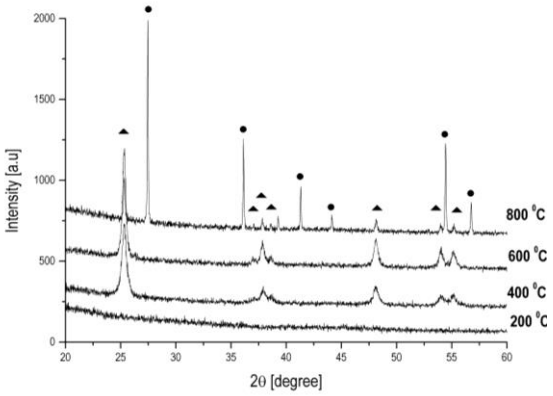

Fig. 1. XRD patterns of TiO_2 powders annealed at 200 ^{0}C, 400 ^{0}C, 600 ^{0}C and 800 ^{0}C for 1h (▲ anatase, ● rutile).

At 200 ^{0}C an amorphous phase was obtained. After heat treatment at 400 ^{0}C and 600 ^{0}C, only an anatase crystalline phase was stabilised and at 800 ^{0}C, 53 % of anatase phase was transformed into rutile phases. In alkaline medium, the anatase crystalline phase was formed due to the lower surface free energy, compared with the surface energy of the rutile crystalline phase [14].

The structural parameters calculated by Rietveld refinement, using the Powder Cell software [7] are presented in Table 1.

Table 1. Structural parameters of TiO_2 samples calculated by Rietveld refinement, using the Powder Cell software.

Sample	Crystalline phases/ Fraction mass [%]		Average crystallite size [nm]		Strain		Lattice parameters [Å]			
	Anatase	Rutile	Anatase	Rutile	Anatase	Rutile	Anatase PDF 21-1272		Rutile PDF 21-1276	
							a	c	a	c
							3.7852	9.5139	4.5933	2.9592
TiO_2 200 ^{0}C	amorphous		-	-	-	-	-	-	-	-
TiO_2 400 ^{0}C	100	-	29	-	0.00637	-	3.7831	9.4804	-	-
TiO_2 600 ^{0}C	100	-	32	-	0.00365	-	3.7881	9.5032		
TiO_2 800 ^{0}C	47	53	73	128	0.00097	0.00065	3.7848	9.4894	4.5801	2.9516

It can be seen that the average crystallite size increased with the increase of calcination temperature due to the agglomeration of particles and/or crystal growth. With the increase of calcination temperature, a narrowing of the elemental cell on c-axis and a decrease of the strain was observed due to transformation of the anatase into rutile, namely the transformation of the anatase body-centred lattice into rutile primitive lattice which involves the breaking and the reforming of the bonds [14,15].

3.2. Raman spectroscopy

Fig. 2 presents the Raman spectra of the samples annealed at different temperatures. Samples treated at 200 ^{0}C can be associated with an amorphous phase of titanium dioxide. The symmetric model of a tetragonal anatase phase were identified at ~144 cm^{-1} (Eg), 197 cm^{-1} (Eg), 398 cm^{-1} (B1g), 515 cm^{-1} (B1g) and 638 cm^{-1} (Eg) [16] for the samples treated at 400 and 600 ^{0}C. For the sample treated at 800 ^{0}C fundamental vibration modes for rutile phase at 446 cm^{-1} and 609 cm^{-1} and the anatase modes were observed [17]. The results obtained by Raman spectroscopy confirm the results from XRD analysis.

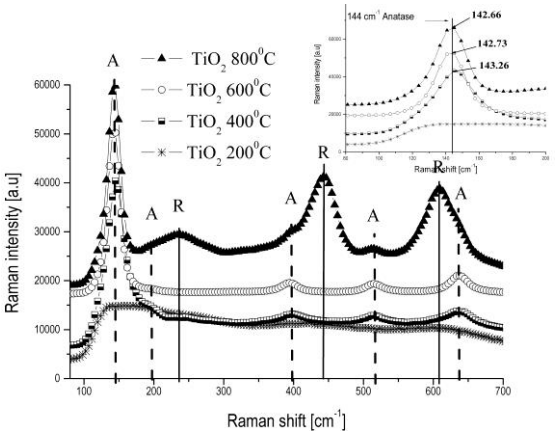

Fig. 2. Raman spectra of TiO_2 powders annealed at different temperatures. Insert: Raman shift of anatase peak position from 144 cm^{-1}.

From the insert in Fig. 2 it was observed that with the increase of the calcination temperatures, the bulk anatase Raman peak position shifted from 144 cm^{-1} to a lower wavenumber which can be correlated with the increase of the lattice deformation induced by the transformation of anatase into rutile [18,19].

3.3. UV-Vis spectroscopy

The absorption spectra of TiO_2 samples annealed at different temperatures are presented in Fig. 3. A red-shift of the absorption edge was observed with an increase of the heat treatment temperature, attributed to an increase of the crystallite size [5,21].

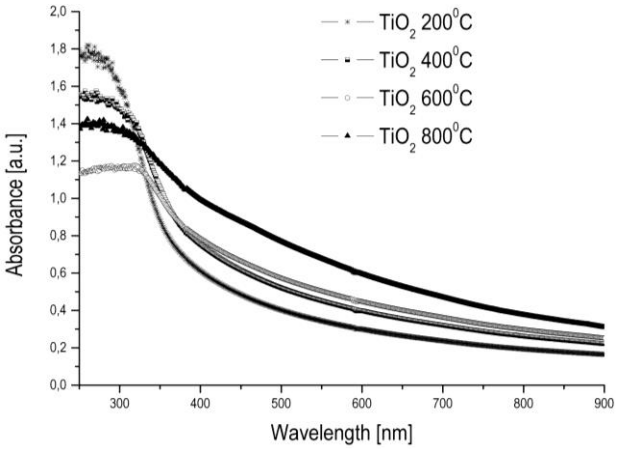

Fig. 3. Absorption spectra of the TiO_2 samples synthesised at pH 8.5 and annealed at different temperatures.

The energy band gap (Fig. 4) decreased from 3.47 eV, for the sample treated at 400 ^{0}C to 2.87 eV for the sample treated at 800 ^{0}C, due to the increase of grain size and the transformation of anatase into rutile [5,21]. The energy band gap of the amorphous titanium dioxide, treated at 200 ^{0}C, was 3.47 eV.

The determination of the Urbach energy is presented as an insert of Fig. 4. The energy band gap and Urbach energy values are presented in Table 2.

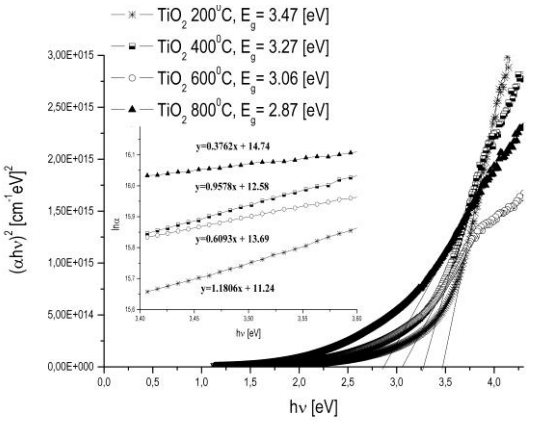

Fig. 4. The determination of the energy band gap of TiO_2 samples annealed at different temperatures. Insert: Determination of Urbach energy.

Table 2. Energy band gaps and Urbach energy of the TiO_2 samples annealed at different temperatures.

Sample	Energy band gap [eV]	Urbach energy [meV]
TiO_2 200 ^{0}C	3.47	847
TiO_2 400 ^{0}C	3.27	1044
TiO_2 600 ^{0}C	3.06	1641
TiO_2 800 ^{0}C	2.87	2658

An increase of the Urbach energy values with annealing temperature can be observed with the lattice deformation caused by the phase's transformation [22].

3.4. Photodegradation process

The photodegradation process of the Methylene Blue dye in the presence of the TiO_2 suspensions, under both UVA and visible irradiation, are shown in Fig. 5. High photocatalytic activity of amorphous TiO_2 can be explained by the higher surface area of the powder with a higher number of active centres [5]. For the sample treated between 400 and 800 ^{0}C, the photo-catalytic activity increased with increase of the calcination temperature, due to the transformation of anatase into rutile, which has the energy band gap smaller than anatase [23].

The efficiency of the photodegradation of Methylene Blue increased from 29% in presence of TiO_2 treated at 400 ^{0}C to 47% for the sample traded at 800 ^{0}C. Even though at 800 ^{0}C, 53% of the anatase is transformed into rutile, the sample exhibits the highest photo-catalytic activity due to the decrease of the energy band gap to 2.89 eV the material could absorb some of the visible radiation.

The variation ln(C/Co) vs. time, assuming that the photodegradation reaction is described after a first order kinetic, is presented in Fig. 6.

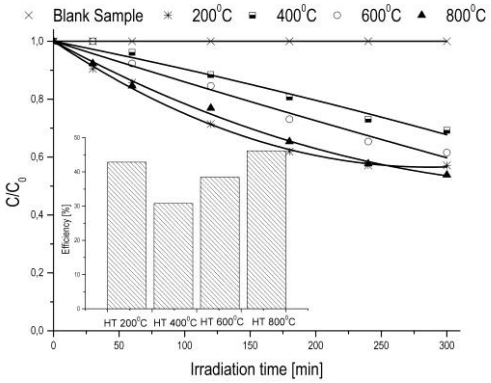

Fig. 5. Photodegradation of Methylene Blue in the presence of TiO_2 catalysts. Insert: The efficiency of photodegradation process, under UV and visible irradiation, after 300 minute.

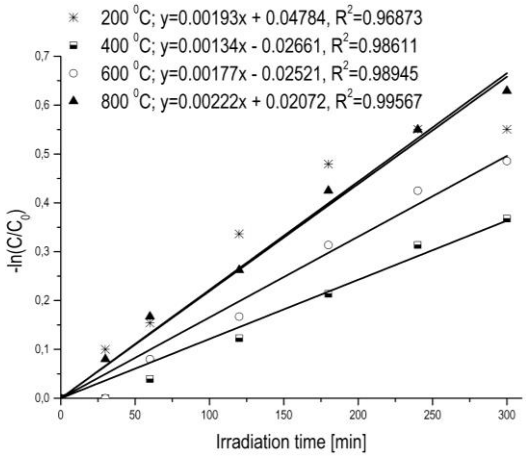

Fig. 6. First order kinetic reactions of the photodegradation of Methylene Blue in presence of TiO_2 annealed at different temperatures.

Based on the kinetic model, the rate constant, k, of the photodegradation process was determined. It can be observed that the rate constant increased from 1.34×10^{-3} in presence of TiO_2 treated at 400 ^{0}C to 1.77×10^{-3} in presence of TiO_2 treated at 600 ^{0}C. The strain decreased with the increase of the calcination temperature (Table 1) from 0.006373 for the sample treated at 400 ^{0}C to 0.003657 for the sample treated at 600 ^{0}C. A decrease of the strain lead to an increase of the rate constant due to the increase of the crystallisation grade of the anatase phase, the photodegradation process is favoured by an increase of crystallinity [24].

4. Conclusion

Titanium dioxide powders were successfully synthesised by a simple hydrolysis method, using titanium tri-chloride as an inorganic precursor. During the annealing temperature studies, it was observed that at a

heat treatment temperature of 200 ^{0}C an amorphous phase of TiO_2 was obtained. At calcination temperatures between 400 and 600 ^{0}C only an anatase crystalline phase was stabilised. The results obtained by XRD were confirmed by Raman spectroscopy. With an increase of heat treatment temperature to 800 ^{0}C a large proportion of the anatase (53 %) is transformed into rutile. Also, based on the XRD data, it was observed that with an increase of heat treatment temperature, the average crystallite size increase, the micro-strain decreased while the lattice deformation increased. The energy band gap decreased with the increase of the annealing temperature from 3.47 eV for the amorphous TiO_2 sample, to 2.87 eV for the TiO_2 sample treated at 800 ^{0}C, while the Urbach energy increased with increase of calcination temperature from 847 meV for the amorphous sample to 2658 meV for the sample treated at 800 ^{0}C. The photodegradation results indicated that all the TiO_2 samples exhibit photo-catalytic activity, even when the intensity of the lamps radiation were low, but the TiO_2 samples which contained both anatase and rutile crystalline phases (sample treated at 800 ^{0}C) exhibits the highest photocatalytic activity due to the lower energy band gap. The efficiency of the photodegradation of Methylene Blue in presence of TiO_2 treated at 800 ^{0}C was ~ 47% under the UVA and visible irradiation, after 300 minutes. The amorphous TiO_2 sample has higher photo-catalytic activity than the anatase phase obtained at 400 ^{0}C, with an efficiency of degradation of dye of 43%.

It can be concluded that it is possible to obtain catalysts with a high photocatalytic performance at low temperatures, even if the powders are amorphous, which leads to a low energy consumption and low cost for the implementation at industrial scale.

Acknowledgment

This paper was supported by the Post‑Doctoral Programme POSDRU/159/1.5/S/137516, project co‑funded from European Social Fund through the Human Resources Sectorial Operational Program 2007‑2013.

References

[1] T. X. Liu, F. B. Li, X. Zh. Li, J. Hazard. Mater. **152**(1), 347 (2008).
[2] Y. Shiraishi, N. Saito, T. Hirai, J. Am. Chem. Soc. **127**, 12820 (2005).
[3] B. Ohtani, Y. Ogawa, S. Nishimoto, J. Phys. Chem. B **101**, 3746 (1997).
[4] J. Zou, J. Gao, F. Xie, J. Alloy. Compd. **497**, 420 (2010).
[5] Q. Wang, X. Chen, K. Yu, Yi Zhang, Y. Cong, J. Hazard. Mater. **246–247**, 135 (2013).
[6] Z. Abbas, J. P. Holmberg, A. K. Hellstriom, M. Hagstrom, J. Bergenholtz, M. Hassellov, E. Ahlberg, Colloid. Surface A **384**, 254 (2011).
[7] W. Kraus, G. Nolze, J. Appl. Crystallogr. **29**, 301 (1996).
[8] J. Tauc, R. Grigorovici, A. Vancu, Phys. Status Solidi. **15**, 627 (1966).
[9] N. Serpone, D. Lawless, R. Khairutdinovt, J. Phys. Chem. **99**, 16646 (1995).
[10] S. H. Kang, J. W. Lim, H. S. Kim, J. Y. Kim, Y. H. Chung, Y. E. Sung, Chem. Mater. **21**, 2777 (2009).
[11] C. H. Ao, S.C. Lee, Chem. Eng. Sci. **60**, 103 (2005).
[12] M. Mohseni, F. Taghipour, Chem. Eng. Sci. **59,** 1601 (2004).
[13] N. Talebian, M. R. Nilforoushan, Thin Solid Films **518**, 2210 (2010).
[14] D. A. H. Hanaor, C. C. Sorrell, J. Mater. Sci. **46**, 855 (2011).
[15] M. Batzill, E. H. Morales, U. Diebold, Phys. Rev. Lett. **96**, 026103 (2006).
[16] S. Balaji, Y. Djaoued, J. Robichaud, J. Raman Spectrosc. **37**, 1416 (2006).
[17] R. Parra, M.S. Goes, M. S. Castro, E. Longo, P. R. Bueno, J. A. Varela, Chem. Mater. **20**, 143 (2008).
[18] A. Golubovic, M. Scepanovic, A. Kremenovic, S. Askrabic, V. Berec, Z. Dohcevic-Mitrovic, Z.V. Popovic, J. Sol-Gel Sci. Technol. **49**, 311 (2009).
[19] D. Bersani, P.P. Lottici, J. Sol-Gel Sci. Technol. **13**, 849 (1998).
[20] P. Davit, G. Martra, S. Coluccia, J. Jap. Petrol. Inst. **47(6)**, 359 (2004).
[21] C. K. Lee, D. K. Kim, J. H. Lee, J. H Sung, I. Kim, K. H. Lee, J. W. Park, Y. K. Lee, J. Sol-Gel Sci. Technol. **31**, 67 (2004).
[22] S. H. Kang, J.-W. Lim, H. S. Kim, J.-Y. Kim, Y.-H. Chung, Y.-E. Sung, Chem. Mater. **21**, 2777 (2009).
[23] H. Xie, L. Zhu, L. Wang, S. Chen, D. Yang, L. Yang, G. Gao, H. Yuan, Particuology **9**, 75 (2011).
[24] M. Inagaki, R. Nonaka, B. Tryba, A. W. Morawski, Chemosphere **64**, 437 (2006).

*Corresponding author: violeta.popescu@chem.utcluj.ro